IEEE Access
Multidisciplinary ⋮ Rapid Review ⋮ Open Access Journal

Received 6 December 2022, accepted 21 December 2022, date of publication 30 December 2022,
date of current version 13 January 2023.

Digital Object Identifier 10.1109/ACCESS.2022.3233465

APPLIED RESEARCH

Optimization Control of Thermal Efficiency for Cement Raw Meal Pre-Decomposition Based on Two-Layer Structure Model Predictive Control

HENGCHAO MA, ZHAO LIU, XIAOHONG WANG, AND HONGHAO MA
School of Electrical Engineering, University of Jinan, Jinan 250022, China

Corresponding author: Zhao Liu (cse_liuz@ujn.edu.cn)

This work was supported in part by the Scientific and Technological SMEs Innovation Ability Improvement Project of Shandong Province under Grant 2022TSGC1081.

ABSTRACT A two-layer structure model predictive control (MPC) for the low thermal efficiency of cement raw material pre-decomposition is proposed. In the upper layer, an outlet temperature of the precalciner automatic setting scheme is formulated with craft constraints by taking advantage of the energy flow and thermal energy conversion models. In the lower layer, the stable control of the precalciner is achieved using a model predictive control algorithm. Finally, extensive simulation results verify the proposed two-layer MPC approach with excellent performance in energy saving and consumption reduction of raw meal pre-decomposition link.

INDEX TERMS Two-layer structure model predictive control, precalciner, energy flow model, thermal energy conversion model.

I. INTRODUCTION

In light of the increasingly stringent environmental policy, research and applications on the digital and intellectual transformation of the cement industry have received substantial interest. Depending on the technology, the process of burning cement clinker can be broken down into the linkages of raw meal pre-decomposition, clinker calcination, and clinker cooling. The coal consumed during the raw meal pre-decomposition link accounts for approximately 60% of the total coal consumed during clinker calcination. Since the precalciner is the most critical equipment in the raw meal pre-decomposition chain and the principal location for raw meal carbonate decomposition, its outlet temperature setting and operation stability impact the energy consumption of the complete clinker calcination process and the quality of the cement clinker. Indeed, the temperature regulation of the precalciner has received substantial attention due to the significant inertia, long-time delay, and strong coupling concerns. For instance, He and Zuo employ a proportional-integral-derivative (PID) control scheme to automate the precalciner's outlet temperature regulation, thereby reducing the operator's burden [1], [2]. Ma used fuzzy control to enhance the precalciner's control automation and better stabilize the outlet temperature than human control [3]. Wang created a precalciner temperature control system based on a fuzzy PID algorithm that outperforms conventional PID and fuzzy control systems in dynamic performance [4]. Currently, the control algorithms listed above are the most prevalent in the cement sector. However, these control algorithms do not consider real-time optimization, making it challenging to meet the enterprises' energy-saving and consumption-reduction objectives. Nevertheless, the two-layer structure model predictive control technique is widely utilized in the petrochemical, thermal power plant, and other industries due to its superior optimization and control performance [5], [6], [7], [8], [9]. Therefore, to satisfy the process and equipment requirements, this work develops a two-layer predictive control model, which optimizes the precalciner's outlet temperature in real-time.

The associate editor coordinating the review of this manuscript and approving it for publication was Guillermo Valencia-Palomo.

II. THE PRE-DECOMPOSITION PROCESS OF CEMENT RAW MEAL

The two main production equipment for raw material pre-decomposition are suspension preheaters and precalciner,

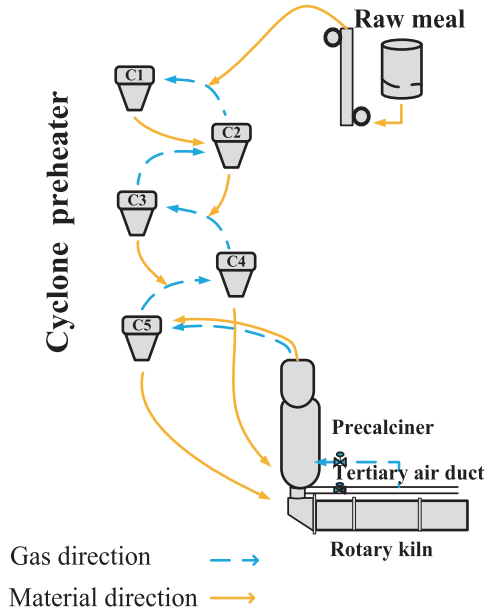

FIGURE 1. Flow chart of cement raw meal pre-decomposition.

with the technological process depicted in Fig.1. Among them, the cyclone preheater comprises five cyclones series, i.e., C1, C2,. . . , and C5, with its primary function being material dispersion, gas-solid heat exchange, and a small portion of calcium carbonate breakdown. In actual production, the raw meal is delivered from the raw meal silo to the junction of the C1 and C2 cyclones using a bucket elevator. Then the high-temperature gas from the C2 cyclone is blown from the bottom to the top into the C1 cyclone to separate the gas from the solid. The raw meal enters the connecting pipe between the C2 and C3 cyclone separators via the air gate valve at the bottom of C1 and is then blown into the C2 cyclone by the high-temperature gas from the C3 cyclone. After layer-heating, the raw meal's moisture is evaporated, and the clay minerals are dehydrated and decomposed, laying a solid foundation for the future decomposition of calcium carbonate and clinker calcination. Finally, the raw material is delivered into the precalciner from the bottom of C4 following preheating at a high temperature.

III. DIFFICULTIES ANALYSIS OF PRECALCINER OUTLET TEMPERATURE CONTROL

The analysis in Section II reveals that timely optimization and accurate control of the precalciner outlet temperature play a crucial role in improving the thermal efficiency of the raw food pre-decomposition link. Currently, the most challenging aspect of controlling the precalciner outlet temperature is the severe coupling of all links, which is easily impacted by the kiln tail coal supplied, the raw material quantity, and the tertiary air from the grate cooler.

A. INFLUENCE OF THE COAL INJECTION AT KILN TAIL

The heat released by coal injection at the kiln tail is the primary heat source of the raw material decomposition. Under the condition that the tertiary air volume remains unchanged, increasing the amount of coal injection at the kiln tail will easily increase the CO2 concentration, resulting in insufficient combustion of pulverized coal in the furnace, and even leading to the "temperature upside down" phenomenon, which affects the equipment's safety. Suppose the injection of coal is lowered. In such a scenario, the precalciner's outlet temperature will decrease, the rate of the raw material decomposition will reduce, and the rotary kiln's load will increase.

B. INFLUENCE OF THE RAW MATERIAL QUANTITY

Clinker yield can be improved by increasing the raw material input after stabilizing the system. However, if the amount of feed is excessive, the balance in the furnace will be disturbed, decreasing the precalciner outlet temperature and the raw material decomposition rate and thus affecting the clinker quality. If the feeding amount is too little, the raw materials in the furnace will undergo excessive decomposition, leading to equipment crusts and other safety hazards.

C. INFLUENCE OF THE TERTIARY AIR

Tertiary air is a high-temperature gas with a temperature above 900°C formed by the grate cooler to cool the clinker. These hot gases enter the precalciner through tertiary air ducts, providing much heat for the precalciner and promoting the combustion of pulverized coal in the furnace. Nevertheless, the valve opening of the tertiary air almost remains unchanged in actual production, and therefore the tertiary air temperature significantly influences the precalciner outlet temperature. If the tertiary air temperature is too low, the outlet temperature of the precalciner will be reduced.

IV. DESIGN OF TWO-LAYER MODEL PREDICTIVE CONTROL STRATEGY

Based on the traditional model predictive control algorithm, the two-layer predictive control introduces a real-time optimization layer, and its structure is shown in Fig.2. It retains the advantages of excellent anti-interference and tracking effect of the traditional model predictive control algorithm, as well as solves problems such as the decline of thermal efficiency and energy waste, due to the untimely and unreasonable artificial control of the precalciner outlet temperature.

A. REAL-TIME OPTIMIZATION LAYER

In order to realize automatic optimal setting of precalciner outlet temperature. In this paper, firstly analyzes the energy flow in the cement raw material pre-decomposition, and then establishes thermal efficiency optimization objective function with the energy conversion model. Finally, the real-time optimization of the precalciner outlet temperature is realized by the particle swarm optimization algorithm.

1) ENERGY FLOW ANALYSIS OF CEMENT RAW MATERIAL PRE-DECOMPOSITION

Energy flow analysis has numerous applications in energy conservation and scheduling in the steel, aluminum,

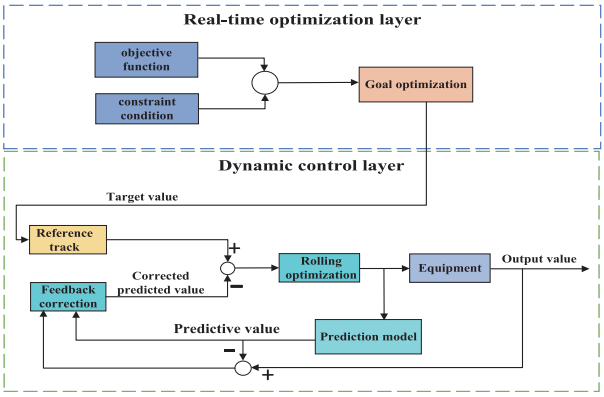

FIGURE 2. Two-layer structure model predictive control structure diagram.

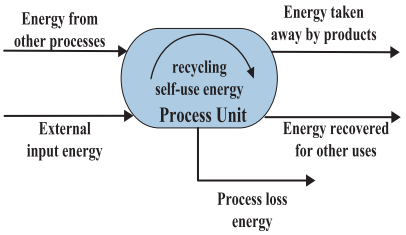

FIGURE 3. Generalized energy flow model.

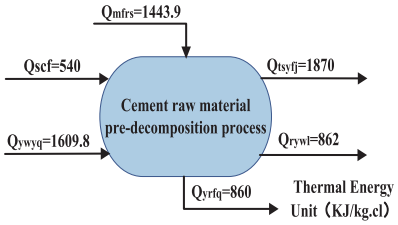

FIGURE 4. Energy flow of raw material pre-decomposition process.

and automotive power design industries, among others [10], [11], [12], [13], [14], [15]. According to diverse sources and orientations, energy in the process industry can be classified as energy from other processes, external input energy, recycling self-use energy, energy taken away by products, energy recovered for other uses, and process loss energy [16], [17], [18]. The model is shown in Fig.3.

According to the above division principles, the energy flow of cement raw material pre-decomposition is shown in Fig.4 (The heat value below 50KJ/kg.cl is not considered). The meaning of parameters is shown in Table 1.

2) ESTABLISHMENT OF THERMAL ENERGY CONVERSION MODEL IN RAW MATERIAL PRE-DECOMPOSITION PROCESS

Under stable working conditions, the conversion relationship between various energies in an industrial production process usually satisfies Equation 1. The conversion model is shown in Fig.5. In (1), Q_{input} is the input energy of the system, α is the energy conversion coefficient, and Q_{output} is the output energy of the system.

TABLE 1. Meaning of energy flow parameters in the raw material pre-decomposition process.

Symbol	Implication	Type	Unit
Q_{mfrs}	The heat released from the combustion of pulverized coal	The external input energy	$KJ/kg\cdot cl$
Q_{scf}	The heat brought in by tertiary air	The energy from other processes	$KJ/kg\cdot cl$
Q_{ywyq}	The heat brought in by kiln tail flue gas	The energy from other processes	$KJ/kg\cdot cl$
Q_{tsyfj}	The heat absorbed by carbonate decomposition.	The energy taken away by the product	$KJ/kg\cdot cl$
Q_{rywl}	The heat taken away by the material entering the rotary kiln	The energy taken away by the product	$KJ/kg\cdot cl$
Q_{yrfq}	The sensible heat for exhaust gas at preheater outlet	The process loss energy	$KJ/kg\cdot cl$

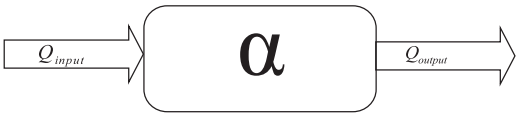

FIGURE 5. Generalized energy conversion model.

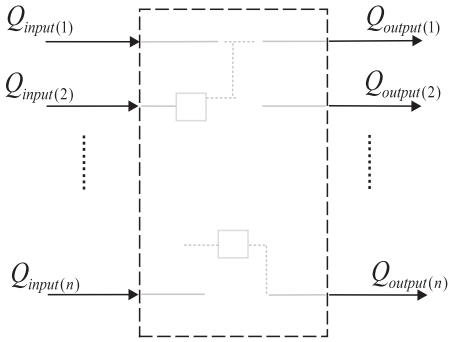

FIGURE 6. Multi-input and multi-output generic energy conversion model.

$$Q_{output} = \alpha \times Q_{input} \tag{1}$$

According to the energy flow analysis in 4.1.1, it can be seen that there are multiple energy inputs and outputs in the raw material pre-decomposition link, so the general energy conversion model can be transformed into Fig.6, where conversion relationship can be expressed by (2). For details of the energy conversion model, please refer to [19].

$$\begin{bmatrix} Q_{output(1)} \\ Q_{output(2)} \\ \vdots \\ Q_{output(m)} \end{bmatrix} = \begin{bmatrix} \alpha_{1,1} & \cdots & \alpha_{m,1} \\ \alpha_{1,2} & \cdots & \alpha_{m,2} \\ \vdots & \ddots & \vdots \\ \alpha_{1,m} & \cdots & \alpha_{m,m} \end{bmatrix} \times \begin{bmatrix} Q_{input(1)} \\ Q_{input(2)} \\ \vdots \\ Q_{input(m)} \end{bmatrix} \tag{2}$$

As shown in Fig.4, although the energy flow of raw material pre-decomposition is multi-input and multi-output, there is only one energy type: heat energy. In constructing the energy conversion model, the following assumptions are consequently made:

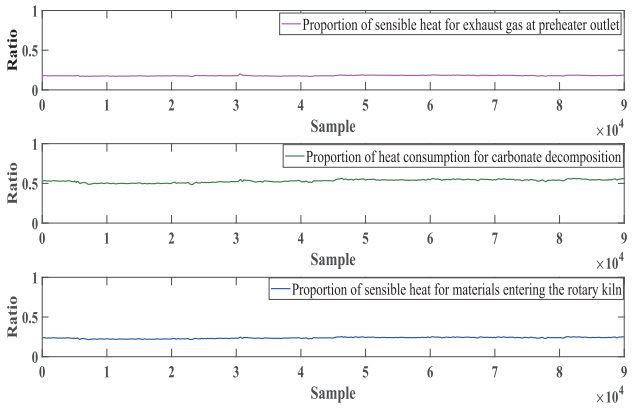

FIGURE 7. Ratio of each thermal energy output to total thermal energy input.

Hypothesis 1: Under stable working conditions, each thermal energy input will supply the same proportion of heat to each thermal energy expenditure item.

Hypothesis 2: According to Hypothesis 1, the proportion formula of thermal energy expenditure as shown in (3) can be established, and the calculation results are shown in Fig.7. In order to improve the calculation accuracy of the model, it is assumed that the conversion coefficient of the heat energy conversion model can be regarded as the ratio of a certain heat energy expenditure to the total heat input, and this value is constant under the steady-state condition.

$$\alpha_i = \frac{Q_i}{Q_{\text{mfrs}} + Q_{\text{scf}} + Q_{\text{ywyq}}} \tag{3}$$

where, α_i is the ratio of thermal energy expenditure; Q_i is the thermal energy expenditure item, $i = 1 \cdots 3$.

Thus, the thermal energy conversion formula of raw material pre-decomposition process can be established as shown in (4).

$$\begin{aligned} Q_{slfj} &= 0.543250 \times (Q_{mfrs} + Q_{scf} + Q_{ywys}) \\ Q_{rywl} &= 0.258207 \times (Q_{mfrs} + Q_{scf} + Q_{ywys}) \\ Q_{yrfq} &= 0.181797 \times (Q_{mfrs} + Q_{scf} + Q_{ywys}) \end{aligned} \tag{4}$$

To determine whether the thermal energy conversion model's assumptions are reasonable, this research picks around 3 hours of continuous production data for simulation verification and calculates the percentage of data error using Formula 5. After the energy conversion model, the percentage error of sensible heat for preheated exhaust gas is less than ±1.5%, the percentage error of heat consumption for carbonate decomposition is less than ±1.2%, and the percentage error of sensible heat for materials entering the rotary kiln is less than±2.5%. The results of the calculations are depicted in Fig.8, The percentage error is less than five percent of the experimental requirements, and the thermal energy conversion model's assumptions are fair.

$$\delta_j = \frac{T_j - t_j}{T_j} \times 100\% \tag{5}$$

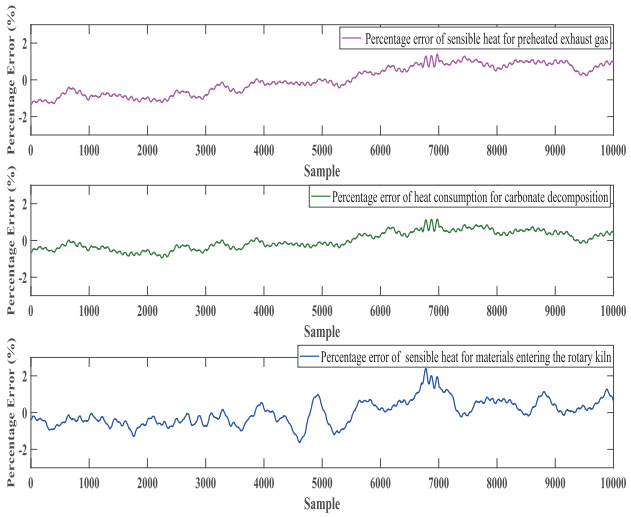

FIGURE 8. Percentage of thermal energy error after conversion.

where, δ_j is the error percentage of the thermal energy conversion model; T_j is the actual heat expenditure of a thermal energy. t_j is the estimated value of a heat energy expenditure after heat energy conversion model; $j = 1 \cdots 3$.

3) ESTABLISHMENT OF THERMAL EFFICIENCY OPTIMIZATION OBJECTIVE FUNCTION

Under stable working conditions, the preheater sensible heat outlet is the largest heat loss source in the process of raw material pre-decomposition. Therefore, reducing the sensible heat of preheated exhaust gas is the most important way to improve the pre-decomposition link thermal efficiency. This paper combined with the ''Methods for the calculation of heat balance, heat efficiency and comprehensive energy consumption of cement rotary kiln'', the following objective function as shown below [20].

$$\begin{aligned} &\min\ Q_{yrfq} = V_{fql} \times C_{fq} \times T_{c1B} \\ &s.t.\ 1.15 \le \frac{M_{sl}}{\rho_{O_2}} \le 1.28^\circ C \\ &\quad 290^\circ C \le T_{c1B} = \frac{Q_{yrfq}}{V_{fql} \times C_{yrfq}} \le 330^\circ C \\ &\quad 85\% \le \eta = \frac{Q_{slfj}}{M_{sl} \times \beta \times \frac{100}{44} \times 1660} \le 95\% \\ &\quad 860^\circ C \le T_{fjl} \\ &\quad = \frac{Q_{rhzywl}}{[(M_{sl} \times \eta \times \beta \times C_1) + (M_{sl} \times (1-\eta) \times C_2)]} \\ &\quad \le 900^\circ C \end{aligned} \tag{6}$$

where V_{fql} is the amount of preheated exhaust gas; C_{fq} is the specific heat capacity of preheated exhaust gas; T_{c1B} is the outlet temperature of the preheater; M_{sl} is the amount of raw material feeding; ρ_{O_2} is the oxygen content in the precalciner; $\eta$is the decomposition rate of raw material; β is the raw material loss on ignition; $C_1$is the specific heat capacity of decomposed raw material;C_2 is the specific heat capacity of undecomposed raw material; T_{fjl} is the precalciner outlet

temperature; 100/44 is the ratio of $CaCO_3$molecular weight toCO_2v molecular weight; 1660 is the unit mass of$CaCO_3$ decomposition energy consumption.

4) SOLUTION OF THERMAL EFFICIENCY OPTIMIZATION OBJECTIVE FUNCTION

At present, there are many optimization algorithms, such as the gradient method, simplex method, and particle swarm optimization [21], [22], [23], [24], [25], [26].The gradient method is generally applicable to unconstrained function optimization problems.The convergence rate of the simplex method is slow when solving functions with constraints. Particle swarm optimization (PSO) is widely presented in many engineering fields because of its simple structure and fast convergence speed. The PSO algorithm is inspired by the natural foraging activity of birds. In the algorithm, flock members are replaced by particles. Each particle has its own speed and position. During the optimization process, each particle continuously updates its own position and speed until it gets the optimal solution that meets the conditions. The optimization process is shown in Fig.9. The updating formula of particle speed and position is shown in (7).

$$V_i(k+1) = wV_{\mathrm{i}}(k) + \mathrm{c}_1\mathrm{r}_1(P_{ibest}(k) - Y_i(k)) + c_2r_2(P_{\mathrm{gbest}}(k) - Y_i(k))$$
$$Y_i(k+1) = Y_i(k) + V_i(k+1) \tag{7}$$

In Equation 7, w is the inertia weight, Y_{i} is the current position of a particle i, V_{i} is the current velocity of the particle, P_{ibest} is the current optimal position of a particle i, and P_{gbest} is the optimal global position of all particles at moment t; c_1,c_2 is the learning factor, and r_1, r_2 is a random number within [0,1]. The value of w is essential to PSO, and there are usually two kinds of fixed and variable values. After simulation, it can be known that the algorithm with a fixed value is 0.5s-1s faster than the algorithm with a variable value, so this paper selects the particle swarm optimization algorithm with a fixed value of w.

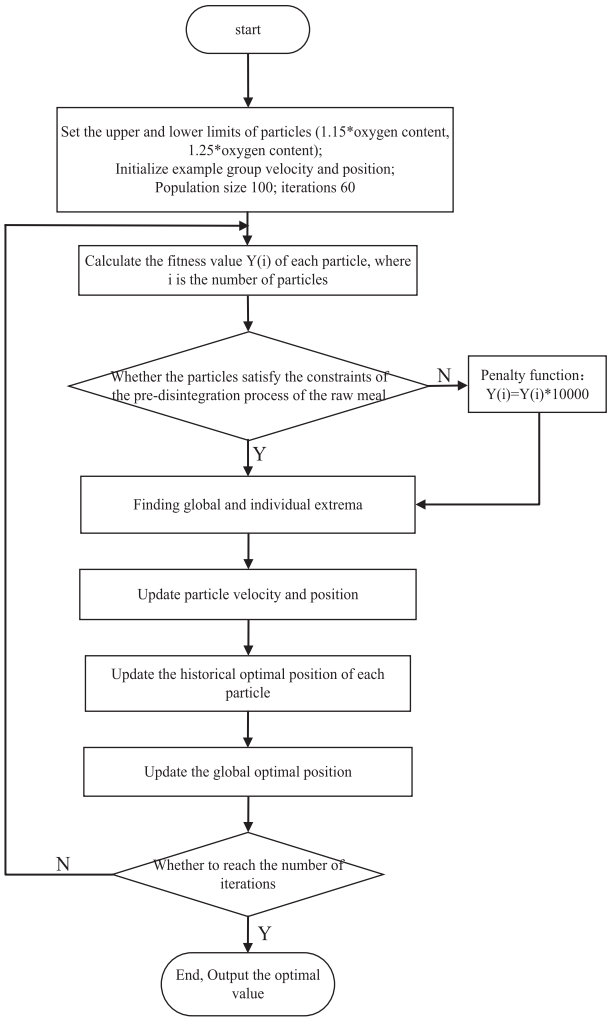

FIGURE 9. Flow chart of particle swarm optimization search.

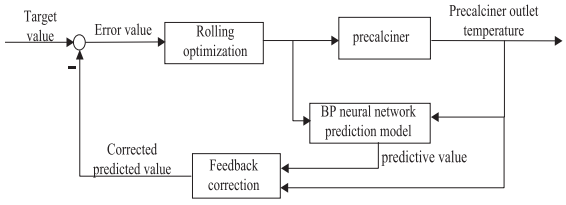

FIGURE 10. Precalciner outlet temperature model prediction control structure diagram.

B. DYNAMIC CONTROL LAYER

As a representative of advanced process control, the MPC has been widely used in complex industrial processes because of its advantages, such as low computational effort and high robustness [27], [28], [29], [30]. Fig.10 depicts the construction of the MPC system, which consists of three components: prediction model, rolling optimization, and feedback correction.

1) PREDICTIVE MODEL

Predictive model serve to predict future outputs based on historical information and future inputs. Since raw material decomposition and pulverized coal combustion are complex physical and chemical reactions, it is hard to accurately model the precalciner outlet temperature input and output through mechanism modeling. This article uses a Back Propagation (BP) neural network to predict the precalciner outlet temperature due to its strong generalization capabilities. Depending on the length of the forecast, the prediction model can be classified into single-step prediction and multi-step prediction. In this paper, a recursive multi-step prediction model with the structure given in Fig.11 and the derivation formula shown in Equation 8 is employed for the multi-step prediction of the

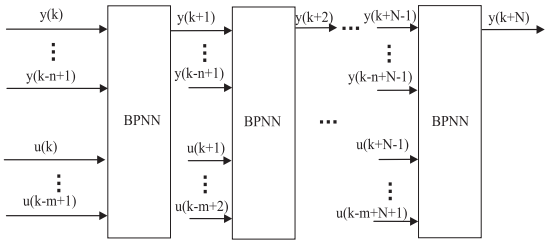

FIGURE 11. Recursive multi-step prediction structure.

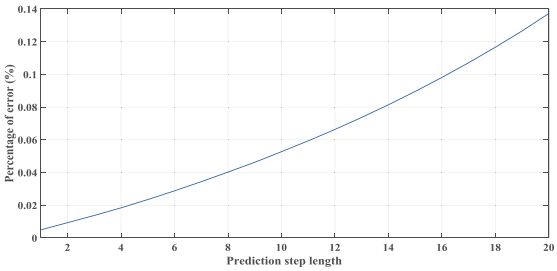

FIGURE 12. Multi-step prediction error percentage.

TABLE 2. Value of multi-step prediction error percentage.

Predicted step size	Percentage of error	Predicted step size	Percentage of error
1	0.0049%	11	0.059%
2	0.0093%	12	0.066%
3	0.0137%	13	0.074%
4	0.018%	14	0.081%
5	0.023%	15	0.09%
6	0.029%	16	0.098%
7	0.034%	17	0.107%
8	0.04%	18	0.117%
9	0.046%	19	0.127%
10	0.053%	20	0.137%

system.

$$\begin{cases} \hat{y}(k+1) = f_{\text{bpnn}} & [y(k), \cdots, y(k-n+1), \\ & u(k), \cdots, u(k-m+1)] \\ \vdots & \\ \hat{y}(k+i) = f_{bpnn} & [y(k+i-1), \cdots, y(k+i-n), \\ & u(k+i-1), \cdots, u(k+i-m)] \\ \vdots & \\ \hat{y}(k+N) = f_{bpnn} & [y(k+N-1), \cdots, y(k+N-n), \\ & u(k+N-1), \cdots, u(k+N-\text{m})] \end{cases} \tag{8}$$

where, f_{bpnn} is the BP neural network, $\hat{y}(k+i)$ is the predicted output at the moment $k+i$, n is the output order of the system, m is the input order of the system, and N is the step size of the prediction.

The prediction error percentage is shown in Fig.12 and Table 2. Although the error increases with the increase of the prediction step, the maximum percentage error is 0.137%, which is lower than the error requirement of the temperature sensor and satisfies the algorith's conditions.

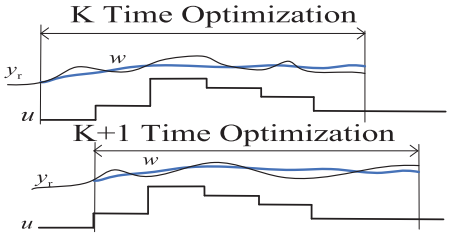

FIGURE 13. Rolling optimization schematic.

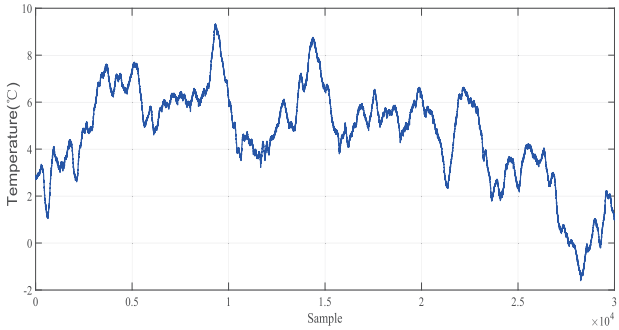

FIGURE 14. Preheating exhaust gas temperature reduction.

2) ROLLING OPTIMIZATION

Rolling optimization aims to use optimization indicators to calculate the future M control increments, so that the predicted value y_r of the next P period is as close as possible to the target value w. This is a rolling optimization in a finite time domain, as seen in Fig.13 At each sampling moment, the optimization performance index only involves a limited time in the future from that moment, and the optimization period of the following sampling moment is moved forward simultaneously. Thus optimization is not performed offline at one time but iteratively online in predictive control.

The optimized performance metrics are shown below:

$$\min J(k) = \sum_{i=1}^{P} q_i[w(k+i) - y_r(k+i)]^2 \times \sum_{j=1}^{M} r_j[(u(k+j) - u(k+j-1)]^2 \tag{9}$$

where, q_i and r_i represent the weight coefficients, P and M represent the optimized and control time-domain lengths, respectively. $w(k+i)$ is the objective value computed by the real-time optimization layer, $y_r(k+i)$ is the anticipated value at time $k+i$, and $u(k+j)$ is the control quantity at time $k+j$ as determined via rolling optimization.

3) FEEDBACK CORRECTION

After the predictive control algorithm determines a series of future control actions through optimization to prevent model mismatch or environmental disturbances from causing the control to deviate from the ideal state, only the control action at the current moment is realized. Before a new optimization is done, the actual output of the object is checked at the next sampling moment, and model-based predictions are corrected

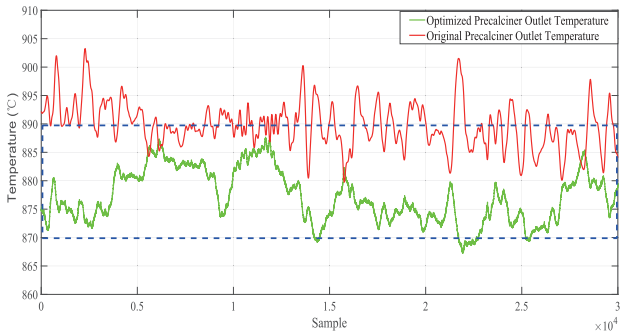

FIGURE 15. Comparison of precalciner outlet temperature before and after optimization.

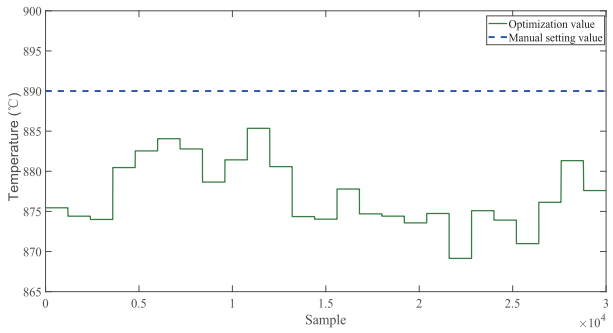

FIGURE 16. Precalciner outlet temperature setting.

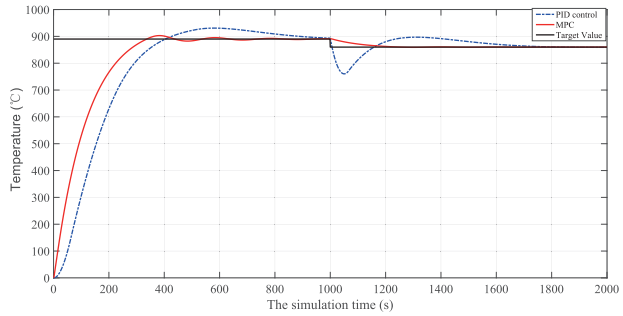

FIGURE 17. Dynamic performance of PID control and MPC systems.

using real-time data. In this paper, the error $e(k)$ is determined by comparing the actual system output $y(k)$ to the predicted output $y_{\mathrm{m}}(k)$:

$$e(k) = y(k) - y_m(k) \tag{10}$$

The reference output is then corrected using $e(k)$:

$$y_r(k+i) = y_m(k+i) + \delta e(k) \tag{11}$$

where, δ is the correction factor, and $y_r(k+i)$ is used instead to achieve rolling optimization and complete the feedback correction.

V. SIMULATION

A. REAL-TIME OPTIMIZATION LAYER SIMULATION ANALYSIS

Fig.14 depicts the optimized preheater output temperature reduction value after roughly 8 hours of simulation, which is generally lower than the temperature before optimization

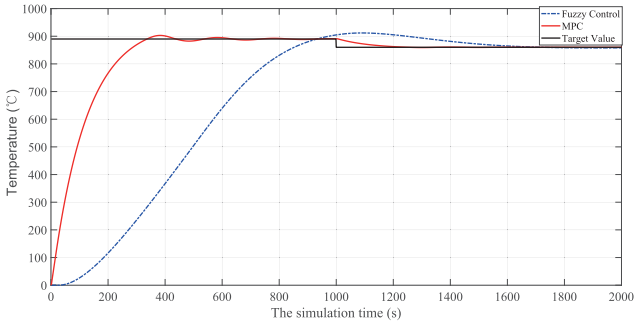

FIGURE 18. Dynamic performance of Fuzzy control and MPC systems.

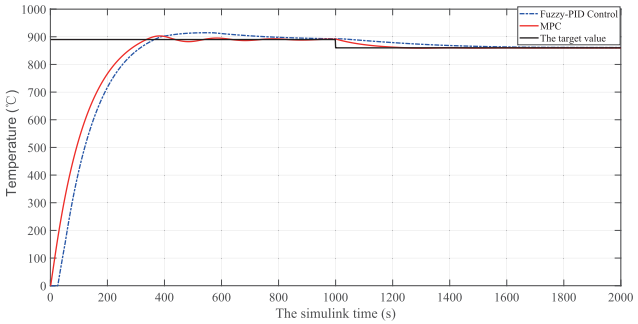

FIGURE 19. Dynamic Performance of Fuzzy-PID control and MPC systems.

and can be decreased by up to 9°C. The precalciner outlet temperature is depicted in Fig.15; following optimization, the temperature changes smoothly and satisfies the process specifications of 870°C—890°C.

The simulation results indicate that this solution positively impacts the energy consumption of the pre-decomposition of raw materials link. Given the large inertia and hysteresis characteristics of the precalciner, to avoid system instability caused by frequent changes in setting values, the temperature adjustment cycle of the precalciner is set to 20 minutes, and the temperature setting curve of the precalciner outlet is shown in Fig.16. In the current actual production, the precalciner outlet temperature does not attract the operator's attention, and according to the data collected in the database, it can be seen that the precalciner outlet temperature is always 890°C. Although this way of setting can lower the operator's work intensity, it also causes reduces thermal efficiency to some degree. In contrast to artificial adjustment, the precalciner outlet temperature setting technique described in this study is more compliant with energy conservation and consumption reduction needs.

B. MODEL PREDICTIVE CONTROL SIMULATION ANALYSIS

Actual mathematical model of the controlled item is necessary for the MPC simulation. In order to simplify the system model, this research uses the kiln tail coal feed as input and the precalciner outlet temperature as output. Utilizes the MATLAB system identification toolbox to identify the transfer function of the decomposer system, as indicated in (12). To evaluate the system's dynamic performance, the simulation time is set to 2000s, and the temperature is set

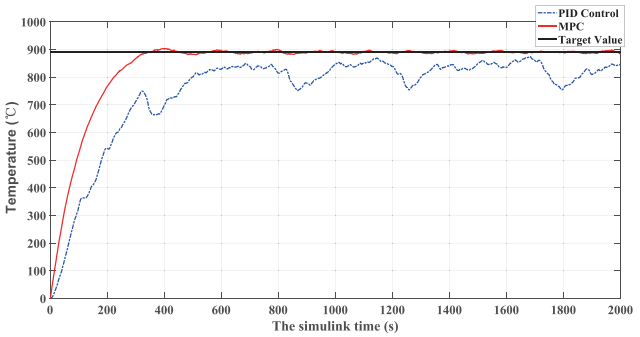

FIGURE 20. Anti-interference performance of PID control and MPC systems.

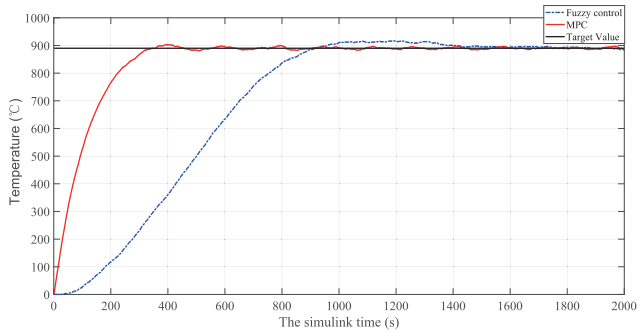

FIGURE 21. Anti-interference performance of Fuzzy control and MPC systems.

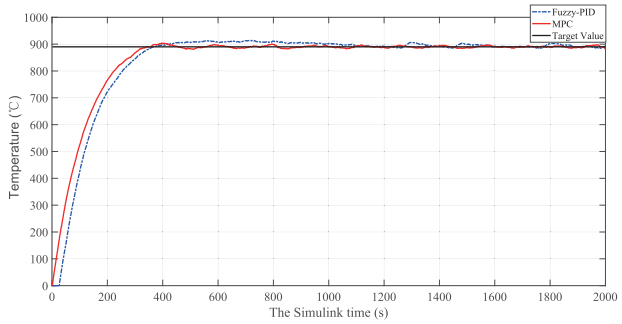

FIGURE 22. Anti-interference performance of Fuzzy-PID control and MPC systems.

to 890°C for the first 1000s and 860°C for the remaining 1000s. The control effect is shown in Fig.17-19. Interference will inevitably occur in the field. In order to test the anti-interference ability of the control system, white noise is introduced in the simulation system, and the effect is shown in Fig. 20-22.

$$G(s) = \frac{109}{120s + 1} \times e^{-26s} \tag{12}$$

According to the simulation data in Table 3, it can be seen that the overshoot of the MPC is 1.4%, which is lower than 4.5% for PID control, 2.5% for fuzzy control, and 2.8% for fuzzy PID control. The settling time is about 300s, which is significantly faster than 650s for PID control, the 1200s for fuzzy control, and 800s for fuzzy PID control. When the setpoint is altered, the MPC has a shorter settling time

TABLE 3. Simulation performance data.

	Model predictive control	PID control	Fuzzy control	Fuzzy-PID control
Overshoot	1.4%	4.5%	2.5%	2.8%
Adjustment time (±2%)	300s	650s	1200s	800s
Steady-state error	0.04°C	0.1°C	0.9°C	0.7°C
Maximum steady-state error after the introduction of disturbances	4°C	System instability	6°C	14°C

and a smoother control process than the other three controls. MPC is more robustness than other control systems when disturbances are introduced.

VI. CONCLUSION

In this paper, a two-layer structure model predictive control strategy is proposed to solve the current situation of low thermal efficiency in the raw material pre-decomposition link. In the real-time optimization layer, the energy flow and thermal energy conversion model of the raw material pre-decomposition process are initially studied to determine the objective function and constraints for thermal efficiency optimization. The optimal precalciner outlet temperature is then calculated in real-time using the particle swarm optimization algorithm, which achieves not only the real-time optimization of the precalciner outlet temperature setting value, but also the energy saving and consumption reduction of the raw material pre-decomposition process. In the dynamic control layer MPC algorithm, a recursive multi-step BP neural network is used to realize a multi-step prediction of the outlet temperature of the resolver. The greatest percentage error of the prediction effect is only 0.137%, which is highly accurate and offers a solid foundation for the MPC algorithm's stability control. Matlab simulation results show that the MPC is better than the more widely used PID, fuzzy control, fuzzy PID and other algorithms in the field in terms of settling time, steady-state error, overshoot, and anti-interference performance, which provides a solid guarantee for the long-term stable and efficient operation of the pre-decomposition link.

REFERENCES

[1] Y. He, "Automatic control function and implementation of decomposition furnace outlet temperature," *Cement Technol.*, no. 2, pp. 49–51, 2015.
[2] Y. T. Zuo, Y. Liu, and H. B. Li, "PID loop for automatic control method of decomposer outlet temperature," *Cement*, no. 10, pp. 62–63, 2015.
[3] Q. H. Ma, X. Shi, and X. C. Hao, "Application of fuzzy control technology on decomposition furnace of jidong cement bishan company," *Cement*, no. 7, pp. 64–67, 2019.
[4] S. H. Wang, Z. F. Wang, and C. H. Jiang, "Fuzzy PID cement decomposer temperature control," *J. Changchun Univ. Technol.*, vol. 37, no. 3, pp. 252–255, 2016.
[5] Q. Ouyang, "Module-based active equalization for battery packs: A two-layer model predictive control strategy," *IEEE Trans. Transport. Electrific.*, vol. 8, no. 1, pp. 149–159, Mar. 2022.

[6] S. Han, J. Shen, L. Pan, L. Sun, and C. Cao, "A L1-LEMPC hierarchical control structure for economic load-tracking of super-critical power plants," *ISA Trans.*, vol. 96, pp. 415–428, Jan. 2020.
[7] H. Sildir, Y. Arkun, A. Ari, I. Dogan, and M. Harmankaya, "Economic model predictive control of an industrial fluid catalytic cracker," *Ind. Eng. Chem. Res.*, vol. 53, no. 45, pp. 17696–17704, Nov. 2014.
[8] E. Aydın, Y. Arkun, and G. Is, "Economic model predictive control (EMPC) of an industrial diesel hydroprocessing plant," *IFAC-PapersOnLine*, vol. 49, no. 7, pp. 568–573, 2016.
[9] L. Wang, "Two-layer structure predictive control and dynamic real-time optimization of large-scale process systems," M.S. thesis, School Econ. Manage., North Univ. Technol., Beijing, China 2019.
[10] M. T. Johansson and M. Söderström, "Options for the Swedish steel industry—Energy efficiency measures and fuel conversion," *Energy*, vol. 36, no. 1, pp. 191–198, Jan. 2011.
[11] M. Yellishetty, P. G. Ranjith, and A. Tharumarajah, "Iron ore and steel production trends and material flows in the world: Is this really sustainable?" *Resour., Conservation Recycling*, vol. 54, no. 12, pp. 1084–1094, Oct. 2010.
[12] S. S. Liu, "Study on the energy flow of aluminum production in China," M.S. thesis, School Electron. Inf. Elect. Eng., Shanghai Jiaotong Univ., Shanghai, China, 2019.
[13] R. Feng, K. Chen, and Z. Sun, "A comparative study on the energy flow of a hybrid heavy truck between AMT and MT shift mode under local driving test cycle," *Energy Convers. Manage.*, vol. 256, Mar. 2022, Art. no. 115359.
[14] Q.-H. Luo and B.-G. Sun, "Experiments on the effect of engine speed, load, equivalence ratio, spark timing and coolant temperature on the energy balance of a turbocharged hydrogen engine," *Energy Convers. Manage.*, vol. 162, pp. 1–12, Apr. 2018.
[15] G. Zhu, J. Liu, J. Fu, and S. Wang, "A combined organic Rankine cycle with double modes used for internal combustion engine waste heat recovery," *J. Eng. Gas Turbines Power*, vol. 139, no. 11, pp. 112804–112812, Nov. 2017.
[16] H. Y. Lin, "Study on energy conversion characteristics and model of continuous casting unit process," M.S. thesis, College Mater. Sci. Eng., Chongqing Univ., Chongqing, China, 2020.
[17] D. Lu, "Energy flow analysis of iron and steel enterprises," M.S. thesis, College Mater. Metall., Liaoning Univ. Sci. Technol., Anshan, China, 2016.
[18] Z. B. Hu and D. F. He, "Research progress of collaborative optimization for material flow and energy flow in steel manufacturing process," *Iron Steel*, vol. 56, no. 8, pp. 61–72, 2021.
[19] M. Geidl and G. Andersson, "Optimal power flow of multiple energy carriers," *IEEE Trans. Power Syst.*, vol. 22, no. 1, pp. 145–155, Feb. 2007.
[20] C. B. M. Federation, "Methods for the calculation of heat balance, heat efficiency and comprehensive energy consumption of cement rotary kiln," China Market Supervision Admin., China Standardization Admin., Tech. Rep. GB/T 26281-2021, China, 2021.
[21] A. T. Khan, X. Cao, Z. Li, and S. Li, "Enhanced beetle antennae search with zeroing neural network for online solution of constrained optimization," *Neurocomputing*, vol. 447, pp. 294–306, Aug. 2021.
[22] L. Zhang and J. Li, "A new globalization technique for nonlinear conjugate gradient methods for nonconvex minimization," *Appl. Math. Comput.*, vol. 217, no. 24, pp. 10295–10304, Aug. 2011.
[23] W. Nakamura, Y. Narushima, and H. Yabe, "Nonlinear conjugate gradient methods with sufficient descent properties for unconstrained optimization," *J. Ind. Manage. Optim.*, vol. 9, no. 3, pp. 595–619, 2013.
[24] N. Vaidya, "Application of quick simplex method on the dual simplex method: A new Approach," *J. Adv. Math. Comput. Sci.*, vol. 24, no. 5, pp. 1–9, Jan. 2017.
[25] D. K. Nadar, "Some applications of simplex method," *Int. J. Eng. Res. Rev.*, vol. 4, no. 1, pp. 60–63, Mar. 2016.
[26] Z. Miao and L. Zhang, "Multi-objective particle swarm optimization algorithm based on competition mechanism," in *Proc. 2nd Int. Conf. Artif. Intell. Educ. (ICAIE)*, Jun. 2021, pp. 150–153.
[27] Z. Z. Chang, M. Li, K. Y. Zhu, M.-J. Sang, and R. Ye, "Model predictive control of long transfer-line cooling process based on back-propagation neural network," *Appl. Thermal Eng.*, vol. 207, May 2022, Art. no. 118178.
[28] D. Muhammad, F. S. Rohman, Z. Ahmad, and N. Aziz, "Low-density polyethylene tubular reactor control using neural Wiener model predictive control," *Asia–Pacific J. Chem. Eng.*, vol. 16, no. 6, pp. 1–18, Nov. 2021.
[29] J. Wang, S. Wei, Q. Wang, and B. Sundén, "Transient numerical modeling and model predictive control of an industrial-scale steam methane reforming reactor," *Int. J. Hydrogen Energy*, vol. 46, no. 29, pp. 15241–15256, Apr. 2021.
[30] L. N. Sridhar, "Multiobjective nonlinear model predictive control of pharmaceutical batch crystallizers," *Drug Develop. Ind. Pharmacy*, vol. 46, no. 12, pp. 2079–2089, 2020.

HENGCHAO MA was born in Tengzhou, Shandong, China, in 1996. He is currently pursuing the master's degree in electronic information with the University of Jinan.

His study focuses on the monitoring and optimization of thermal efficiency in the process industry.

ZHAO LIU was born in Dezhou, Shandong, China. He received the Ph.D. degree in engineering majored in mechanical and electronic engineering from the Shenyang Institute of Automation, Chinese Academy of Sciences, in July 2016.

His research interests include monitoring, analysis, and optimization of energy efficiency in the process industry, and intelligent control of complicated industrial processes.

XIAOHONG WANG is currently a Prominent Specialist of Taishan Scholars in Shandong Province, the Director of the Institute of Automation, University of Jinan, a Ph.D. Advisor, and the Leader of the control theory and control engineering field. He is also the Director of the Robotics Committee of the Chinese Society of Automation, Automation Branch of the China Silicate Society, Shandong Automation Society, and the Shandong Building Materials Industry Integrated Automation Engineering Center. His research interests include advanced control theory and process control field, and has made remarkable achievements in the theoretical research and engineering practice of comprehensive automation in the cement industry.

HONGHAO MA was born in Zaozhuang, Shandong, China, in 1998. He received the bachelor's degree in measurement and control technology and instrument from the University of Jinan, in 2020, where he is currently pursuing the degree in electronic information.

His research interests include process industry automation control and intelligent optimization algorithm.